

Steric and Electronic Effects on the Configurational Stability of Residual Chiral Phosphorus-Centered Three-Bladed Propellers: Tris-aryl Phosphanes

Simona Rizzo,^[d] Tiziana Benincori,^[a] Valentina Bonometti,^[b] Roberto Cirilli,^[c] Patrizia R. Mussini,^[f] Marco Pierini,^[e] Tullio Pilati,^[d] and Francesco Sannicolò*^[f]

Abstract: A series of tris-aryl phosphanes, structurally designed to exist as residual enantiomers or diastereoisomers, bearing substituents differing in size and electronic properties on the aryl rings, were synthesized and characterized. Their electronic properties were evaluated on the basis of their electrochemical oxidation potential determined by voltammetry. The configurational stability of residual phosphanes, evaluated by dynamic HPLC on a chiral stationary phase or/and by dynamic ¹H and ³¹P NMR spectroscopy, was found to be rather modest (barriers

of about 18–20 kcal mol⁻¹), much lower than that shown by the corresponding phosphane oxides (barriers of about 25–29 kcal mol⁻¹). For the first time, the residual antipodes of a tris-aryl phosphane were isolated in enantiopure state and the absolute configuration assigned to them by single-crystal anomalous X-ray diffraction analy-

Keywords: chirality • density functional calculations • electrochemistry • phosphanes • residual stereoisomers

sis. In this case, the racemization barrier could be calculated also by CD signal decay kinetics. A detailed computational investigation was carried out to clarify the helix reversal mechanism. Calculations indicated that the low configurational stability of tris-aryl phosphanes can be attributed to an unexpectedly easy phosphorus pyramidal inversion which, depending upon the substituents present on the blades, can occur even on the most stable of the four conformers constituting a single residual stereoisomer.

Introduction

We have reported the results of an investigation aimed at clarifying the steric and electronic effects on the configura-

tional stability of tris-aryl phosphane oxides existing as residual^[1] stereoisomers, enantiomers or diastereoisomers, in the immediately preceding paper, where the definitions and the basis for the existence of this unique category of stereoisomers devoid of rigid stereogenic elements are exhaustively illustrated.^[2] The research was developed through the following steps: 1) synthesis and structural characterization of a series of tris-aryl phosphane oxides; 2) isolation of the residual stereoisomers through efficient chromatographic separation techniques or by crystallization of conglomerates; 3) assignment of the absolute configuration (P_{res} or M_{res})^[3] to the residual stereoisomers by single-crystal X-ray diffraction analysis or comparison of their chiroptical properties; 4) assessment of the configurational stability of the residual stereoisomers by racemization kinetics followed by off-column chiral HPLC, or by dynamic ¹H and ³¹P NMR spectroscopic analysis; 5) evaluation of the electronic availability of the systems by voltammetric methods; 6) theoretical investigation on the electronic property–configurational stability relationships.

All of the residual phosphane oxides were found to be configurationally stable compounds displaying quite high activation energies for the helix reversal process which controls the configurational stability of residual three-bladed propellers (the so-called M_0 stereoisomerization mechanism).^[3] The barrier is comprised between 25 and 29 kcal mol⁻¹. Most importantly, the results of this investigation clearly proved that configurational stability is primarily dependent on steric factors, although also electronic contribu-

[a] Prof. T. Benincori
Dipartimento di Scienza e Alta Tecnologia
Università degli Studi dell'Insubria
via Valleggio 11, 22100 Como (Italy)

[b] Dr. V. Bonometti
Dipartimento di Chimica
Università degli Studi di Milano
via Golgi 19, 20133 Milano (Italy)

[c] Dr. R. Cirilli
Dipartimento del Farmaco, Istituto Superiore di Sanita',
Viale Regina Elena, 299, 00161 Roma (Italy)

[d] Dr. S. Rizzo, Dr. T. Pilati
Istituto di Scienze e Tecnologie Molecolari
Consiglio Nazionale delle Ricerche, via Golgi 19, 20133 Milano
(Italy)

[e] Prof. M. Pierini
Dipartimento di Chimica e Tecnologie del Farmaco
Università di Roma "La Sapienza"
P.le Aldo Moro 5, 00185 Roma (Italy)

[f] Prof. P. R. Mussini, Prof. F. Sannicolò
Dipartimento di Chimica and C.I.M.A.I.N.A.
Università degli Studi di Milano,
via Golgi 19, 20133 Milano (Italy)
Fax: (+39) 02-50314139
E-mail: francesco.sannicolò@unimi.it

Supporting information for this article is available on the WWW under <http://dx.doi.org/10.1002/chem.201201182>.

tions from the substituents present on the aromatic rings were shown to play a role in modulating the barrier of the M_0 process, especially those related to the rigidity of naphtho-condensed five-membered 1,3-dioxolane or six-membered 1,4-dioxane rings.

The primary aim of this paper is to extend the research to tris-aryl phosphanes designed to exist as residual stereoisomers, and again investigate how steric and electronic factors, related to the nature of tailored substituents present on the blades, could influence their configurational stability. Electronic effects were evaluated by comparing the results obtained in the case of substrate **1b**, taken as reference, and phosphanes **1d**, wherein an electron-releasing ethoxyl group is present, and **1c** carrying an electron-withdrawing sulfo group. The substituents should show merely electronic effects, since they are located in the 6-position of the naphthalene rings, which is not involved in the dynamic gearing of the blades (Figure 1).

The importance of steric effects could be estimated in the case of substrates **1a**, **1b**, **2a**, **2b**, and **3** (Figure 1). In the case of **2b**, one of the two equatorial methyl groups located on the 1,4-dioxene ring should play an important role in increasing the engagement of the blades and hence their degree of correlated rotation. Furthermore, the two *trans*-diequatorial methyl groups block dioxene ring flipping and thus increase its rigidity and hence the steric hindrance. Two residual diastereoisomers are expected in this case, since the stereogenicity of the six carbon stereocenters (all *S*) combines with residual stereogenicity. A somewhat lower degree of dynamic blade gearing was expected for **3**, in which the methyl groups on the five-membered 1,3-dioxolene ring are farther from the crucial core of the propeller than those located in the 2-position of the six-membered dioxene ring.

Results and Discussion

Synthesis of the phosphanes: Phosphanes **1b** and **2a** were already described previously.^[3] Sulfonation of **1b** with 20% oleum in sulfuric acid solution at 0°C afforded **1c** in excellent yield.

Phosphane **1a** was prepared by reaction of the Grignard derivative of 1-bromo-2-methoxynaphthalene with PCl_3 . Analogously, **1d** was obtained by re-

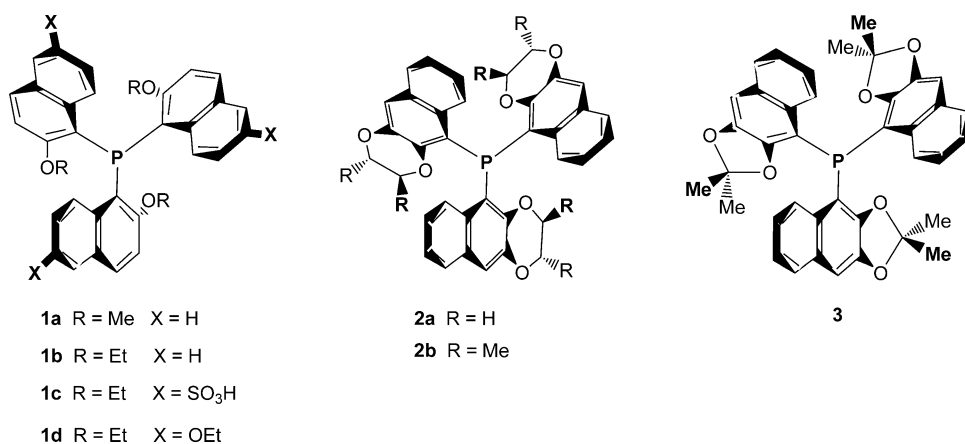


Figure 1. The series of tris-aryl phosphanes investigated in the present work.

action with PBr_3 of the Grignard derivative of 1-bromo-2,6-diethoxynaphthalene, obtained in turn by bromination of 2,6-diethoxynaphthalene, synthesized by alkylation of 2,6-dihydroxynaphthalene with bromoethane in basic medium, with *N*-bromosuccinimide (NBS).

A diastereomeric mixture of phosphanes **2b** was synthesized by reaction of the lithium derivative of (2*S*,3*S*)-5-bromo-2,3-dimethylnaphtho[2,3-*b*]-1,4-dioxene with PCl_3 in refluxing THF solution. The latter was prepared by bromination of (2*S*,3*S*)-2,3-dimethylnaphtho[2,3-*b*]-1,3-dioxene with NBS in 50% acetic acid/chloroform solution. Some 5,10-dibromo derivative was formed, which was removed by column chromatography. (2*S*,3*S*)-2,3-Dimethylnaphtho[2,3-*b*]-1,4-dioxene was prepared by reaction of 2,3-dihydroxynaphthalene with the ditosylate of commercially available enantiopure (2*R*,3*R*)-2,3-butanediol in pyridine solution. Double configuration inversion was demonstrated by single-crystal X-ray anomalous scattering analysis of the bromo derivative (Figure 2).

Phosphane **3** was synthesized by reaction of the lithium derivative of 4-bromo-2,2-dimethylnaphtho[2,3-*d*]-1,3-dioxole with PCl_3 in refluxing THF solution. The bromo derivative was prepared by bromination of 2,2-dimethylnaphtho[2,3-*d*]-1,3-dioxole with NBS in 50% acetic acid/chloroform solution. Some 4,9-dibromo derivative was formed which was removed by column chromatography. Phosphane **3** was

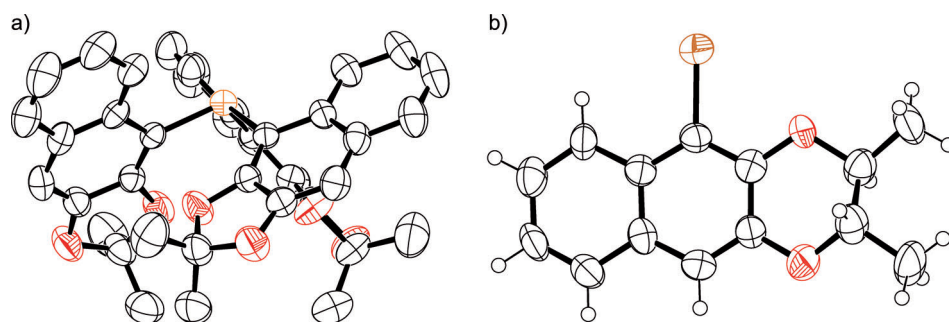


Figure 2. ORTEPs of a) (M_{res})-**3** and b) (2*S*,3*S*)-5-bromo-2,3-dimethylnaphtho[2,3-*b*]-1,4-dioxene. Hydrogen atoms are omitted.

found to crystallize as a conglomerate from ethyl acetate and was resolved into antipodes by fractional crystallization (Figure 2). As far as we know, **3** is the first example of a phosphane existing as residual enantiomers isolated in enantiopure state.

X-ray diffraction data: The crystal structures of **1b** and **2a** were already reported previously.^[3] The ORTEP of (*M*_{res})-**3** is shown in Figure 2. As anticipated, this compound crystallizes as a conglomerate, and thus the absolute configuration could be inferred from anomalous X-ray scattering data.

The conformational situation in the crystal structure of **3** deserves some comments: 1) The preferred conformation of the blades in the crystal is *aaa* (all priority edges of the blades below the reference plane), in accordance with our previous findings for **1b** and **2a**. 2) The C-P-C angles in **3** (av ≈ 103.7°) are very narrow and smaller than those found in the crystal structure of phosphanes **1b** and **2a** (av ≈ 108.5 and 106.1°, respectively), suggesting stronger steric interference amongst the blades of the propeller, with higher rotational gearing and, presumably, higher configurational stability, provided that the *M*₀ mechanism is solely responsible for racemization.

Evaluation of the electronic properties of phosphanes: The electronic properties of phosphanes were evaluated by cyclic voltammetry in MeCN + 0.1 M tetrabutylammonium perchlorate (TBAP) solution, by following the same experimental protocol as in our parallel work on phosphane oxides^[2] (Figure 3). The first oxidation peak (*E*_{p,1a}) can be associated with conversion of the free phosphane to the phosphane oxide. This electron-transfer process appears to be chemically irreversible in the experimental scan-rate range, although some traces of a return peak can be perceived at the highest scan rates *v*, and electrochemically quasireversible (moderate but perceivable shift of the oxidation potential in the positive direction even under ohmic-drop compensation, for example, $dE_{p,1a}/d\log v = 0.024$ V for **1a**).

The first oxidation peak potentials are reported in Table 1 together with the corresponding sums of the Hammett parameters, which, in the case of the substituted 1-bromonaphthalenes corresponding to the blades, account for the inductive effects acting on the carbon atom connected to the phosphorus center.^[2] Plotting the first oxidation peak potentials, against the $\Sigma\sigma_{\text{blade}}$ values gave a fairly linear Hammett relationship (Figure 4), that is, the electron transfer is regularly affected by electronic effects, and increasingly electron poor blades result in regularly increasing energy required to oxidize the phosphorus atom. For the three cyclic diethers, oxidation appears to occur at potentials slightly higher than expected; this could point to some steric hindrance effect, hampering the accessibility of the phosphorus core to the electrode surface. The second oxidation peak potentials are consistent with the first oxidation peak potentials of the corresponding phosphane oxides and substituted 1-bromonaphthalenes corresponding to the blades, and therefore should be ascribed to oxidation of aromatic blades.^[2]

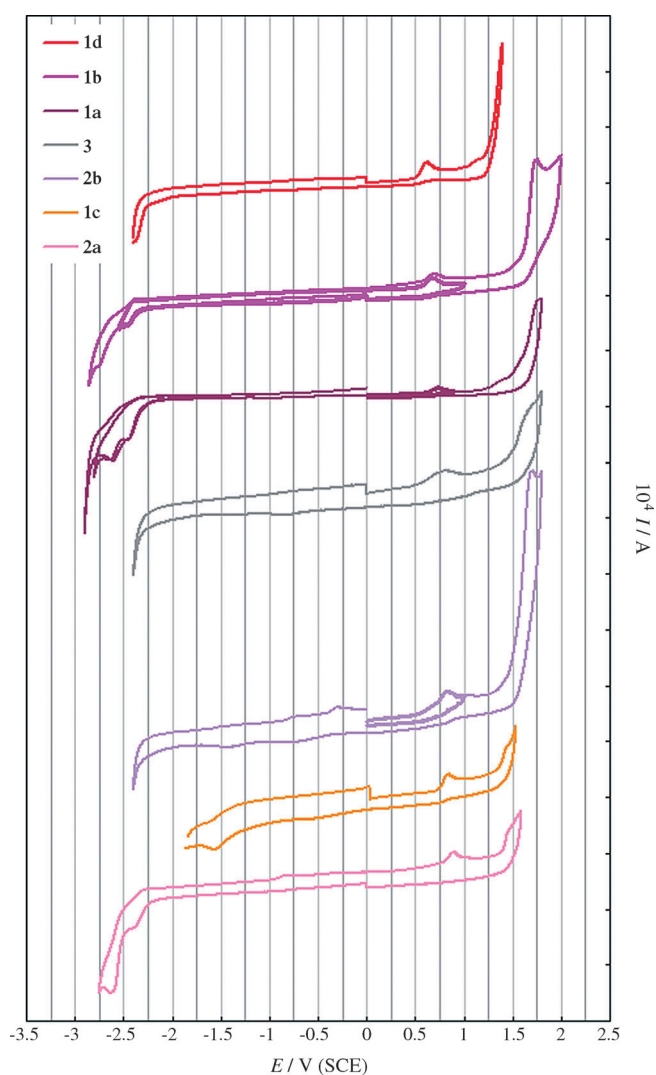


Figure 3. Voltammetric curves of phosphanes in a 10⁻³ M MeCN solution with 10⁻¹ M TBAP as supporting electrolyte.

Table 1. First oxidation peak potentials of phosphanes in MeCN + 10⁻¹ M TBAP solution. The sum of Hammett parameters for the phosphane blades, calculated as detailed in ref. [2] is also reported.

Phosphane	$\Sigma\sigma_{\text{blade}}^{[1]}$	Substituents	<i>E</i> _{p,a (max)}
1d	-0.24	2-OEt, 6-OEt	0.62
1b	0	2-OEt	0.66
1a	0	2-OMe	0.74
3	0.10	2,3-OC(Me) ₂ O	0.78
2b	0.10	2,3-OCH(Me)CH(Me)O	0.82
1c	0.35	2-OtEt, 6-SO ₃ H	0.83
2a	0.12	2,3-OCH ₂ CH ₂ O	0.88

Symmetrically, the perceivable reduction peaks, obtained starting with the reductive scan on the original phosphane, must be ascribed to aromatic-blade reduction. In the case of **1b**, the first one, which appears to be fully reversible and monoelectronic, should correspond to formation of a stable radical anion on one blade; accordingly, the second reduction peak, still monoelectronic and quasireversible, in spite

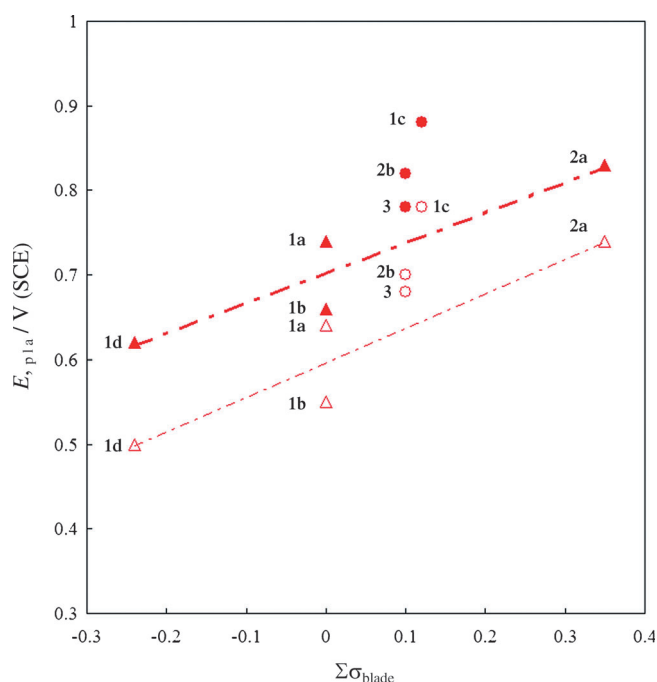


Figure 4. Hammett relationships concerning the first oxidation peak potentials (onset: empty symbols, peak: full symbols) for the phosphane series. Circles denote cases with cyclic diether substituents, and triangles the remaining cases.

of appearing as a shoulder on the background, could correspond to the same process taking place on a second blade (two equivalent but reciprocally interacting redox centers).

Resolution of the residual racemates of phosphanes and evaluation of the enantiomerization and diastereomerization barriers of the residual stereoisomers of phosphanes:

All phosphanes studied in the present investigation were found to be configurationally unstable at room temperature. This precluded the possibility of determining the enantiomerization barriers through techniques involving isolation of the antipodes in an enantiopure state, except for **3**, as anticipated.

Furthermore, the experimental difficulties related to the resolution of the racemates of phosphanes and diphosphanes by HPLC on a chiral stationary phase (CHPLC), even at an analytical level, are well documented. Satisfactory separations are described only in the case of electron-poor systems.^[4] In the case of the residual stereoisomeric phosphanes, these difficulties are superimposed on the low configurational stability. Thus, any at-

tempt at CHPLC resolution had to be performed at very low temperatures, for brief elution times, and on short, high-performance columns.

Despite all these constraints, we were able to achieve good and quick separation of the residual enantiomers of **1a**, **1b**, and **1d** at low temperature ($-20/-25^{\circ}\text{C}$) under conditions that suppress the enantiomerization process completely in the case of **1a** and almost completely in the cases of **1b** and **1d**. The enantioseparations were carried out on Chiralpak IA-3 CSP with a binary mixture composed of pentane and a small percentage of 2-propanol as mobile phase. Taking advantage from the fact that the polysaccharide-derived Chiralpak IA-3 CSP is based on 3 μm particles, we could operate at high flow-rates ($>3\text{ mL}\cdot\text{min}^{-1}$), drastically reducing the elution times without significant loss in efficiency.^[5]

To evaluate the helix inversion barriers by chiral dynamic HPLC^[6a-l] (DHPLC, Figure 5), the enantioseparations were carried out at increasing temperatures. The dynamic chromatograms displayed typical plateau zones between the peaks of the resolved enantiomers, indicative of the fact that partial enantiomerization was taking place during the separation process (Figure 5). Kinetic information relevant to these dynamic events could then be obtained by suitable line-shape analyses.^[6m-u]

In the case of **3**, enantioseparation under the experimental conditions described above was incomplete and thus unsuitable for quantitative evaluation of stereolability by DHPLC (see Supporting Information), whereas the racemates of **1c** and **2a** and the diastereomeric mixture of **2b** were not resolved at all. In spite of these unsuccessful results, we believe that the chromatographic approach presented in this work may not only provide a very effective tool to gain information about the helix inversion barriers of the residual stereoisomers of tris-aryl phosphanes, but also pave the way to enantioseparation of classical phosphanes and diphosphanes.

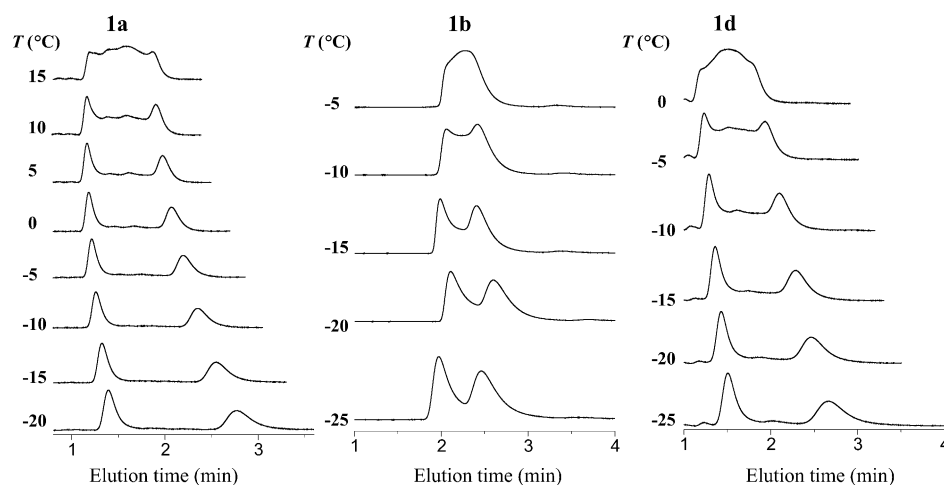


Figure 5. Variable-temperature HPLC of the racemates of phosphanes **1a**, **1b**, and **1d**. Column: Chiralpak IA-3 100 \times 4.6 mm; detector: UV at 254 nm. **1a** and **1d**: eluent: pentane/2-propanol (100/2); flow rate: 4.0 $\text{mL}\cdot\text{min}^{-1}$. **1b**: eluent: pentane/2-propanol (100/0.25); flow rate: 3.0 $\text{mL}\cdot\text{min}^{-1}$.

The complete list of the enantiomerization barriers determined by the DHPLC technique for **1a**, **1b** and **1d** in the whole temperature range from -25 to 10°C is given in Table S1 of the Supporting Information. The helix inversion barriers measured according to these on-column experiments were (18.7 ± 0.1) kcal mol $^{-1}$ for **1a**, (17.9 ± 0.1) kcal mol $^{-1}$ for **1b**, and (17.8 ± 0.1) kcal mol $^{-1}$ for **1d** at -10°C (Table 2).

Table 2. Enantiomerization and diastereomerization energy barriers (ΔG^\ddagger [kcal mol $^{-1}$]) for residual phosphanes (P) and phosphane oxides (PO), $E_{\text{p,a}}$ of the phosphanes, and differences in the enantiomerization or diastereomerization barriers between the phosphanes and the corresponding oxides. Details of all employed Eyring plots are given in the Supporting Information.

Phosphane	$\Delta G^\ddagger_{\text{P}}$ [kcal mol $^{-1}$] [-10°C]	$\Delta G^\ddagger_{\text{P}}$ [kcal mol $^{-1}$] [55°C]	$\Delta G^\ddagger_{\text{P}}$ [kcal mol $^{-1}$] [80°C]	$E_{\text{p,a}}$ (P) [V]	$\Delta G^\ddagger_{\text{PO}}$ [kcal mol $^{-1}$] [55°C]	$\Delta\Delta G^\ddagger_{\text{P-PO}}$ [kcal mol $^{-1}$] [55°C]
1a	18.7 ^[a]	19.9 ^[b]	20.3 ^[b]	–	27.5	7.6
1b	17.9 ^[a]	19.1 ^[b]	19.6 ^[b]	0.68	27.5	8.4
1c	16.3 ^[c]	16.5 ^[e]	16.9 ^[d]	–	–	11.0
1d	16.1 ^[c]	17.1 ^[e]	17.5 ^[d]	0.82	27.0	9.9
2a	17.9 ^[a]	18.8 ^[b]	19.2 ^[b]	0.62	28.6	9.8
2a	–	–	–	0.88	27.8	–
(P_{res})- 2b	16.9 ^[e]	18.1 ^[e]	18.5 ^[f]	0.82	29.1	11.0
(M_{res})- 2b	17.6 ^[e]	18.5 ^[e]	18.9 ^[f]	–	30.0	11.5
3	18.1 ^[c]	19.0 ^[e]	19.4 ^[d]	0.78	25.4	6.4

[a] Determined by DHPLC. [b] Extrapolated through Eyring plot based on DHPLC data. [c] Extrapolated through Eyring plot based on ^1H DNMR data. [d] Determined by ^1H DNMR spectroscopy. [e] Extrapolated through Eyring plot based on ^{31}P DNMR data. [f] Determined by ^{31}P DNMR spectroscopy.

In the case of **1b**, the DHPLC investigation was coupled with dynamic ^1H NMR experiments (DHNMR) by analyzing the progressive coalescence of the signals of the diastereotopic hydrogen atoms of the methylene groups of the three homotopic ethoxyl groups at increasing temperatures ranging from 40 to 100°C (Figure 6c). The enantiomerization barriers measured for **1b** on the basis of these experiments were in quite good agreement with the equivalent values extrapolated at the same temperatures from the data obtained by on-column enantiomerization experiments, especially in the light of the different solvents employed for the two techniques (i.e., pentane/2-propanol 100/2 or 100/0.25 as the mobile phase in DHPLC experiments and $[\text{D}_6]$ DMSO in the DHNMR studies, Table S1 of the Supporting Information).

Analogous DHNMR experiments were carried out for nonresolvable sulfonated phosphane **1c** (Figure 6a). The barriers inferred from these experiments, carried out in $[\text{D}_6]$ DMSO solution and in the temperature range from 60 to 120°C , were very close to those determined for **1b** by using the same technique and moderately lower than those determined for **1a**, **1b**, and **1d** by DHPLC measurements (Table S1 of the Supporting Information). The DHNMR method was employed also for **3**, in which two geminal diastereotopic methyl groups are present (Figure 5b). The enantiomerization barriers measured in $[\text{D}_6]$ DMSO from 80 to 130°C proved to be a little higher than those found for the other phosphanes (Table S1 of the Supporting Information).

As anticipated, resolution of **3** was achieved taking advantage of the fact that it crystallizes as a conglomerate. In this case, it was possible to record the CD spectra of both enantiomers of **3** at -10°C (Figure 7a) and to assign them the absolute configuration P_{res} or M_{res} . The CD spectrum of the (M_{res})-**3** enantiomer (Figure 2) displayed a weak negative band located around 260 nm followed by a more intense positive CD signal at 240 nm. A computational simulation of the electronic CD spectra of the enantiomers of **3** reproduced satisfactorily the experimental CD profiles (see Experimental Section and Supporting Information for details) and matched the absolute configuration assignment achieved by the X-ray diffraction method.

We also took advantage of the availability of enantiopure samples of **3** to evaluate the configurational enantiolability of this phosphane by CD signal decay at 240 nm (Figure 7b). The racemization barrier measured by this method in CHCl_3 solution was (18.1 ± 0.2) kcal mol $^{-1}$ at -10°C , in complete agreement with the equivalent value extrapolated at the same temperature from the DHNMR data (Figure 6b).

Since an effective chromatographic system for the direct separation of the two residual diastereoisomers of **2b** is not available, we evaluated the helix inversion barriers by dynamic ^{31}P DNMR coalescence experiments on the phosphorus signals (Figure 8). The diastereomerization barriers of **2b** calculated from these coalescence experiments were 18.53 kcal mol $^{-1}$ at 80°C for the conversion of the less stable (P_{res})-**2b** into the more stable stereoisomer (M_{res})-**2b**, and 18.85 kcal mol $^{-1}$ for the opposite process.

All of the Eyring plots are characterized by very good correlation coefficients and are coherently in agreement with the monomolecular nature of the monitored stereomutations. They indicated very low values of activation entropy (ΔS^\ddagger), which lie between 14 and 19 entropic units (Table S1 of the Supporting Information). In addition, the activation enthalpies (ΔH^\ddagger) were found in a very narrow range from 11.4 to 14.4 kcal mol $^{-1}$, which suggests that they may be the expression of a very similar stereoisomerization mechanism.

On the whole, these results give indirect evidence for the reliability of the data, which therefore can be confidently employed to gain effective indications for comparing the configurational stability of the tris-aryl phosphanes under investigation. To facilitate the comparison, the enantiomerization and diastereomerization energy barriers, the $E_{\text{p,a}}$ values, and the barriers of the corresponding oxides are reported in Table 2. These data highlight two interesting points: the phosphanes are about 10 kcal mol $^{-1}$ less stable than the corresponding oxides, and the barriers are rather similar in all cases (the difference between the lowest and the highest helix inversion barrier is less than 3 kcal mol $^{-1}$), independent of steric and electronic factors. For example, at the selected temperature of 55°C (the same value as in the kinetic measurements performed on the related phosphane oxides),^[2] the

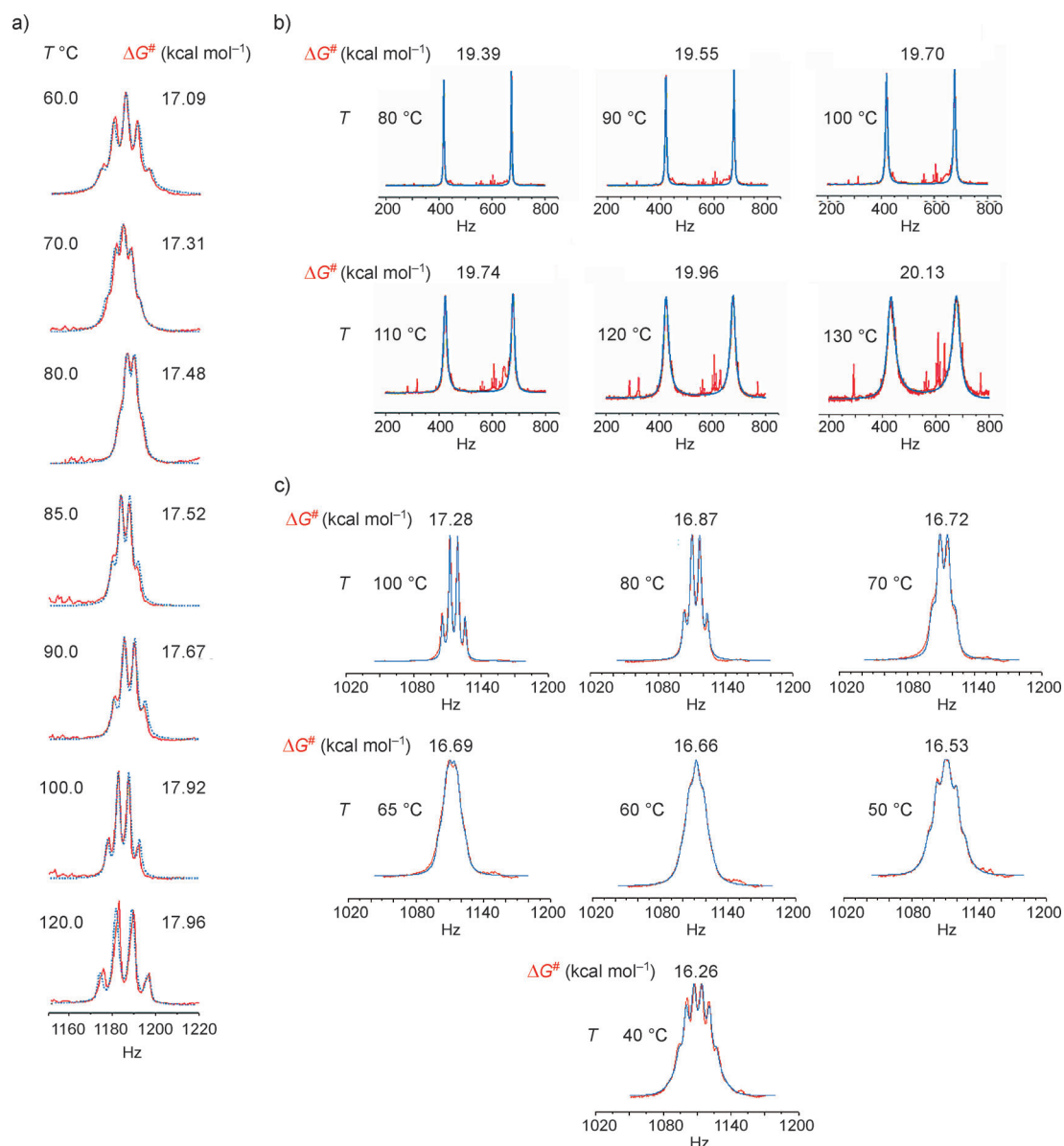


Figure 6. Dynamic ^1H NMR spectra ($[\text{D}_6]\text{DMSO}$) at different temperatures of the racemates of phosphanes; simulated spectrum in blue, experimental spectrum in red. a) Compound **1c**: signals of the methylene hydrogen atoms of the ethoxyl groups. b) Compound **3**: signals of the methyl groups. c) Compound **1b**: signals of the methylene hydrogen atoms of the ethoxyl groups.

most sterically hindered phosphane **2b** displays stereoisomerization barriers ($\Delta G^\ddagger = 18.1/18.5 \text{ kcal mol}^{-1}$) which are close to (even lower) than that of the much less congested **1a** ($\Delta G^\ddagger = 19.9 \text{ kcal mol}^{-1}$). Furthermore, the barrier found for **1b** [$\Delta G^\ddagger = 19.1 \text{ kcal mol}^{-1}$ (DHPLC)] is practically unaffected by introduction of an electron-releasing group, like in **1d** [$\Delta G^\ddagger = 18.8 \text{ kcal mol}^{-1}$ (DHPLC)], and only modestly reduced by introduction of an electron-withdrawing substituent, like in **1c** [$\Delta G^\ddagger = 17.1 \text{ kcal mol}^{-1}$ (DHNMR)].

Considering that the gearing of the three blades should be more pronounced in phosphanes than in phosphane oxides, as suggested by the X-ray data, we felt forced to consider for phosphanes an enantiomerization/diastereomerization path alternative to the M_0 mechanism invoked for the ster-

eoisomerization of the tris-aryl phosphane oxides. The most obvious suggestion is that tris-aryl phosphanes could undergo phosphorus pyramidal inversion, which is precluded in the case of the phosphane oxides. This hypothesis appeared, however, not so easy to accept, since the racemization barrier of some chiral enantiopure aryl phenyl ethyl phosphanes was found to lie in the range of 28–34 kcal mol^{-1} , depending on the electronic properties of the substituents present on the aryl groups,^[7] and then, at least in principle, it did not seem reasonable to accept such a dramatic drop of 15 kcal mol^{-1} for tris-aryl phosphanes. To shed some light on this point, we performed theoretical calculations to investigate the dynamics of tris-aryl phosphanes.

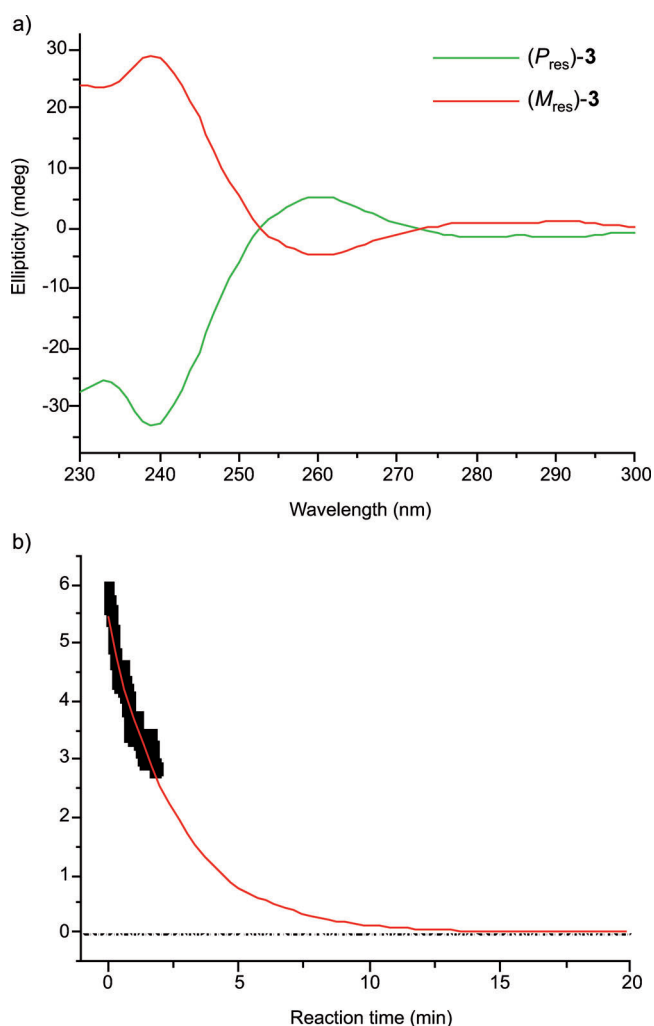


Figure 7. a) CD spectra of the enantiomers of **3** in CHCl_3 solution at -10°C . b) CD signal decay at -10°C monitored at 240 nm.

Theoretical calculations: Considering the very large number of structures we planned to optimize in both ground and transition states, special attention was devoted to the choice of a quantum mechanical modeling method suitable for quantitative estimations of phosphorus inversion barriers (with deviations from the experimental value of 2–3 kcal mol⁻¹) in variously substituted phosphanes with acceptably short computation times.

The hybrid Hartree–Fock/DFT method B3LYP with 6-31G(d) basis set proved to be quite a good compromise to obtain the desired accuracy of the kinetic data at a reasonable computational expense. Indications of the adequacy of this approach were achieved by calculating the phosphorus inversion barriers of the three phosphanes **6–8** (Figure 9), two of which have a phenyl group bonded to the phosphorus atom, and comparing the calculated results with the experimentally determined inversion barriers reported in the literature. The calculated-versus-experimental standard deviation was 0.8 kcal mol⁻¹, and the greatest absolute errors associated with the two phenyl-substituted phosphanes **7** and **8**

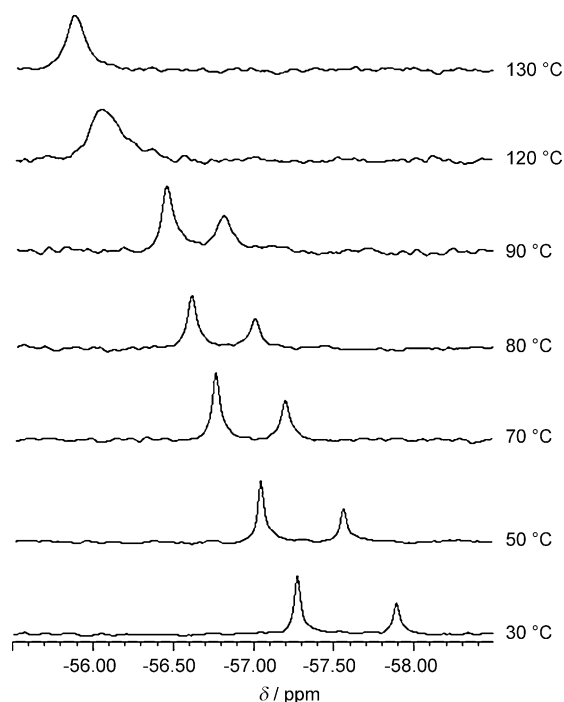


Figure 8. ³¹P NMR spectra at different temperatures of the diastereomeric mixture of P_{res} and M_{res} phosphanes **2b** in $[\text{D}_6]\text{DMSO}$.

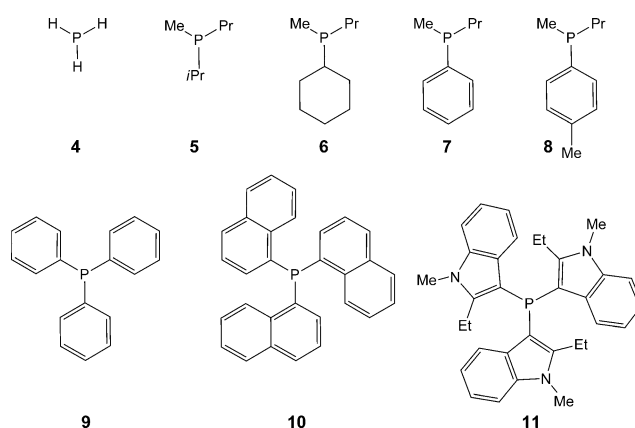


Figure 9. Structures of the phosphanes used as models in quantum mechanical calculations.

were only 0.2 kcal mol⁻¹ (Table 3). These results enabled us to extend the same method to some of the tris-aryl phosphanes studied in this work, as well as to others employed as models (compounds **4**, **5**, **9–11**^[11] in Figure 9).

The data in Table 3 clearly predict a progressive decrease in the activation barrier for phosphorus inversion (P inversion) on increasing the number of aromatic rings bonded to the same phosphorus atom. This is particularly evident in the 5 kcal mol⁻¹ drop in the barrier on substituting the isopropyl or cyclohexyl group of **5** and **6**, respectively, with a phenyl group to give phosphane **7**. An additional decrease of 2 kcal mol⁻¹ was then predicted for P inversion in compound **8**, obtained by formal exchange of the *n*-propyl fragment in **7** with a phenyl group. A further reduction of 4 kcal

Table 3. Calculated parameters for phosphanes.

	LPF ^[a]	O–C ₃ axis ^[b]	C–P–C ^[c]	$\Delta E^{\ddagger}_{\text{P-inv}}$ ^[d]	$\Delta E^{\ddagger}_{M_0}$ ^[e]	ΔG^{\ddagger} ^[e]	$\Delta E^{\ddagger}_{\text{Lit.}}$ ^[g]
(<i>M</i> _{aaa})- 1a	–	1.90	108.1	16.9	24.5	19.3 ^[h]	–
(<i>M</i> _{aaa})- 1b	–	1.99	108.5	14.3	25.8	18.6 ^[h]	–
(<i>M</i> _{aaa})- 2b	–	2.06	108.6	16.3	–	17.5 ^[h]	–
(<i>P</i> _{aaa})- 2b	–	2.03	108.6	17.2	–	18.1 ^[h]	–
(<i>M</i> _{aaa})- 3	–	2.12	105.3	24.1	25.7	18.6 ^[h]	–
(<i>M</i> _{sss})- 3	–	–	108.4	17.0	–	18.6 ^[h]	–
4	2.00	–	93.4	35.5	–	–	34.4, ^[8] 36.7 ^[9]
5	1.40	–	101.3	37.6	–	–	–
6	1.38	–	101.4	37.5	–	36.1 ^[7]	–
7	1.20	–	101.8	32.5	–	32.7 ^[7]	–
8	1.12	–	101.5	31.0	–	30.9 ^[7]	–
9	1.06	–	102.6	26.8	–	–	–
(<i>P</i> _{sss})- 10	1.00	–	102.9	27.3	10.5	–	–
(<i>P</i> _{sss})- 11	–	–	106.1	24.3	13.5	–	25.1 ^[10]

[a] Fraction of lone electron pair still residing on the P atom in the TS of P inversion. [b] Distance [Å] between the C₃ symmetry axis and the O atom in the 2-position of the naphthalene blades. [c] Average C–P–C angle found in the most stable of the optimized stereoisomers of each species and in (*M*_{sss})-**3**. [d] Calculated barriers [kcal mol^{−1}] for the P-inversion process. [e] Calculated enantio- and diastereomerization barriers [kcal mol^{−1}] involved in the M₀ mechanism. [f] Experimental enantiomerization and diastereomerization barriers [kcal mol^{−1}] extrapolated to 25 °C by Eyring plots of experimental data. [h] Calculated P-inversion barriers [kcal mol^{−1}] from the literature. [i] This work.

mol^{−1} was calculated on replacing the methyl group of **8** with a third phenyl group: an inversion barrier of 26.8 kcal mol^{−1} at 25 °C was calculated for triphenylphosphane (**9**). Interestingly, no significant difference in the P-inversion barrier was predicted for **10**, in which the three phenyl groups of **9** have been exchanged with α -naphthyl groups.

The tendency of the phosphorus atom to undergo easier inversion on increasing the number of the aromatic substituents may be interpreted by assuming that the transition states involved in the inversion process can effectively reduce their energy by delocalization of the lone pair from the planar phosphorus toward the aromatic rings. This assumption is consistent with the experimental findings and their interpretation given by Mislow and Baechler,^[7] as well as with the quite modest inversion barriers of acyl phosphanes, for which resonance stabilization of the transition state is assumed to promote their stereolability.^[10]

Convincing theoretical support in favor of this interpretation was obtained by evaluating through quantum mechanical calculations performed on phosphanes **4–10** the phosphorus lone pair fraction (LPF) still residing on the P atom in the HOMO in the planar transition state involved in the P-inversion process (Table 3 and Figure 10). Progressive insertion of new phenyl groups leads to progressive reduction of the LPF to the minimal value of one electron in tris-aryl phosphanes **9** and **10**. However, kinetic processes with free-energy activation barriers greater than 26.5 kcal mol^{−1} at room temperature display half-lives of more than a month, that is, the species involved in such events may be considered virtually stable. Therefore, although tris-aryl phosphanes **9** and **10** were predicted to have much lower P-inversion barriers than any common tris-alkyl phosphanes, their stereolability at room temperature must be assumed to be negligible.

A dramatic reduction of the P-inversion barrier is observed when the naphthalene rings connected to the phosphorus atom carry an additional substituent in the 2-position, like in compounds **1a**, **1b**, **2b**, and **3** (Table 3), though, in the last-named, a strong reduction is predicted only for the *M*_{sss} stereoisomer belonging to the *M*_{res} enantiomer (or conversely for the *P*_{sss} stereoisomer belonging to the *P*_{res} enantiomer). Interestingly, in all cases, a quite wide average C–P–C angle in the phosphanes is associated with a remarkable loss of stereostability. This observation suggests that additive hindrance in the 2-position of the three aromatic blades leads to a more open 3D angle of the pyramidal phosphorus center when the rings are disposed *anti* with respect to the P–LP framework (P–LP = phosphorus lone pair), which therefore becomes more prone to attaining the planar structure required by the transition state leading to inversion.

Particularly interesting is the case of the *P*_{aaa} and *M*_{sss} conformers of **3** belonging to the same *M*_{res} re-

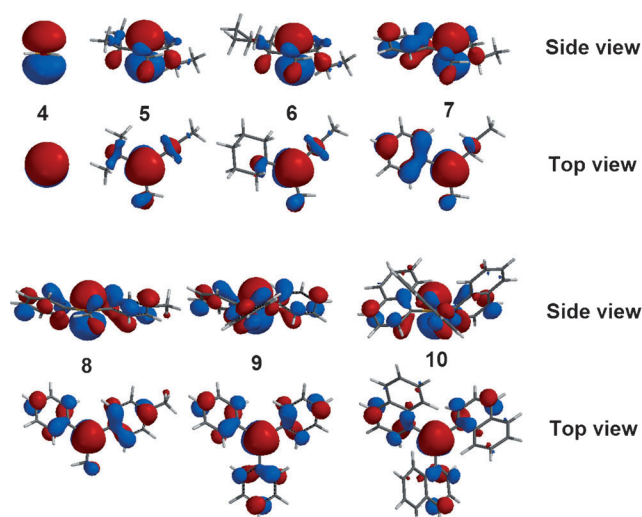


Figure 10. Expansions of lobes constituting the calculated HOMOs in the transition states of P inversion in phosphanes **4–10**.

sidual enantiomer. In contrast to **1a**, **1b**, and **2b**, the *P*_{aaa} geometry, which in **3** is largely the most stable one, has an average C–P–C angle (105.3°) that is much narrower than that of its related stereoisomer *M*_{sss} (108.4°). Therefore, coherent with what was highlighted above, also a much higher P-inversion barrier was assessed for (*P*_{aaa})-**3** (24.1 kcal mol^{−1}) than for (*M*_{sss})-**3** (17.0 kcal mol^{−1}).

By comparison of the (*P*_{aaa})-**3** structure with those of the equivalent *P*_{aaa} (or *M*_{aaa}) stereoisomers **1a**, **1b**, and **2b**, it appears that the narrower C–P–C angles in (*P*_{aaa})-**3** are due to the presence of the small, five-membered dioxolene rings. This strained structure imposes a greater distance of the oxygen atoms in the 2-position of the naphthyl frameworks

from the C_3 symmetry axis characterizing all of the P_{aaa} structures (Table 3). This situation allows closer approach of the blades in (P_{aaa})-**3** to each other, which reduces the 3D angle defined by the phosphorus atom and the three aromatic moieties. Comparison of the P-inversion barriers calculated for **1a**, **1b**, **2b**, and **3** and the experimentally measured activation free energies related to the enantiomerization (**1a**, **1b**, and **3**) or diastereomerization processes [(M_{res})-**2b** and (P_{res})-**2b**] shows that a full compatibility exists between such kinetic data, since the calculated standard deviation is only 2.5 kcal mol⁻¹. Therefore, the helix inversion of the chiral tris-aryl phosphanes studied in this work could be the first reported case of stereoisomerization of residual enantiomers governed by phosphorus pyramidal inversion and not by the M_0 mechanism.

To obtain a convincing conclusion to this topic, we resorted to theoretical calculations. The transition states of the enantiomerization processes occurring by the M_0 mechanism were modeled for **1a**, **1b**, **3**, **10**, and **11**^[11] and then optimized at the B3LYP/6-31G(d) level of theory. The calculations were limited to the most stable stereoisomer of one of the two residual enantiomers. The results of the calculations (Table 3) indicated that the M_0 pathway is favored over P inversion only for tris(1-naphthyl)phosphane (**10**) and for the indolic phosphane **11**, both of which are devoid of appreciable hindrance at the level of the zone *anti* to the P-LP framework in their most stable *sss* conformers (relevant average C-P-C 102.9 and 106.1°, respectively), while it becomes strongly disfavored in **1a** and **1b**, in which additive hindrance is produced in the zone *anti* to the P-LP framework of their most stable *aaa* conformers by the methoxyl and ethoxyl groups, respectively (average C-P-C 108.1 and 108.5°, respectively).

In phosphane **3**, which shows greater similarity to **1a** and **1b** than to **10** and **11**, the assessed energy difference between the two mechanisms is very small, albeit again in favor of P inversion. However, it seems reasonable and possible that, in this case, enantiomerization might switch toward an energetically more favorable multistep pathway, resulting from the connection between the M_1 stereoisomerization mechanism controlling interconversion of the stereoisomers of the same residual enantiomer through very small activation barriers (typically < 10 kcal mol⁻¹) and P inversion. In this way, the most stable (M_{aaa})-**3** conformer may be converted to the less stable (P_{sss})-**3** diastereoisomer through the M_1 mechanism, and then the (P_{sss})-**3** conformer (stereomutation barrier of only 17 kcal mol⁻¹ calculated for this stereoisomer) may be transformed into the opposite residual enantiomer (P_{aaa})-**3** by P inversion. The energetically identical mirror sequence (P_{aaa})-**3** → (M_{sss})-**3** → (M_{aaa})-**3** would be also active.

On the basis of the above considerations, it is also possible to rationalize the lower enantiomerization barrier (ca. 0.8 kcal mol⁻¹) found for phosphane **1b** relative to **1a**, though the former has bulkier ethoxyl groups at the 2-position of the naphthyl moieties. The lower hindrance exerted by the methoxyl groups in **1a** leads to slightly narrower C-

P-C angles (average angle of 108.1° calculated for **1a** versus 108.5° for **1b**) and therefore to a ground state a bit farther from the planar transition state required for P-inversion.

Conclusion

The present investigation has given interesting information on the configurational stability of substituted tris-aryl phosphanes as residual stereoisomers and on the electronic and steric parameters affecting the P-inversion barrier of these compounds. A series of tris-naphthyl phosphanes, designed to exist as residual stereoisomers and differing in electronic and steric properties, has been synthesized and fully characterized. One of them was obtained as a pure enantiomer by fractional crystallization by taking advantage of the information given by X-ray diffraction analysis that the racemic phosphane crystallizes as a conglomerate from dichloromethane/ethyl acetate.

The electronic properties of the phosphanes have been quantitatively evaluated through electrochemical methods. In particular the oxidative peak potentials have been found to be in good agreement with the Hammett polar constants of the substituents on the naphthyl rings.

The racemization barriers have been carefully evaluated by applying different dynamic techniques (¹H DNMR, ³¹P DNMR, and DHPLC on a chiral stationary phase) to the racemates. CD decay kinetics has been coupled with ¹H DNMR experiments in the case of the phosphane isolated as enantiopure antipode. The successful resolution of some racemic phosphanes by HPLC, a technique often found to be unsatisfactory and of very limited scope in the case of chiral phosphanes and diphosphanes, is noteworthy.

All of the phosphanes have been found to be configurationally labile at room temperature, in contrast to the corresponding oxides, which were previously described as configurationally very stable residual stereoisomers under analogous conditions and showed helix reversal barriers of about 25–29 kcal mol⁻¹ at room temperature. The barriers were found to lie in the very narrow range between 18 and 20 kcal mol⁻¹, which suggests different helix reversal mechanism for phosphanes and phosphane oxides. Phosphorus pyramidal inversion, impossible in phosphane oxides, which undergo helicity reversal exclusively through the M_0 mechanism, appeared to be the most probable stereomutation process.

Calculations gave a clear picture of the way in which tris-aryl phosphanes manifest their stereochemical lability. They revealed that the aromatic nature of the phosphorus substituents contributes to reduction of the P-inversion barrier by about 5, 7, and 11 kcal mol⁻¹ for progressive attachment on phosphorus of one, two, and three phenyl groups, respectively, while the exchange of three phenyl groups with naphthyl moieties does not produce significant reductions in the barrier.

Strong promotion of P inversion is triggered by the presence of substituents in the 2-position of the three aromatic

blades. The *aaa* cluttered states force the three C-P-C angles to open, bringing the ground states closer to the planar transition states for P inversion (the reduction in the P-inversion barrier was calculated to range from 10 to 13 kcal mol⁻¹, Table 3). At the same time, the increased steric hindrance in the zone *anti* to the P-LP framework leads to marked destabilization of the transition state involved in the *M*₀ stereoisomerization mechanism (a computed increase in the barrier ranging from 12 to 15 kcal mol⁻¹ for phosphanes **1a**, **1b** and **3**), making this pathway significantly disadvantaged at room or low temperatures.

The diastereomeric phosphanes **2b** are among the most stereolabile phosphanes ($\Delta G^\ddagger = 18.1$ and 18.5 kcal mol⁻¹), since rigid and sterically demanding dimethyldioxene rings facilitate phosphorus inversion. On the contrary, the corresponding oxides, for which inversion is not possible, are the most stable residual stereoisomers ($\Delta G^\ddagger = 29.1$ and 30.0 kcal mol⁻¹), since the same steric congestion produces pronounced blade gearing, which favors the configurational stability of residual stereoisomers.

Thus, it seems reasonable to conclude that any attempt to improve the stereostability of tris-aryl phosphanes by increasing blades engagement by substitution of the positions *ortho* of the aromatic rings in fact inhibits helix reversal by the *M*₀ mechanism; however, it conversely promotes phosphorus inversion, thwarting the original purpose.

Experimental Section

Spectroscopy: The CD spectra and CD decay experiments were carried out by using a Jasco Model J-700 spectropolarimeter. The optical path and temperature were set at 0.1 mm and -10°C. Melting points were measured by Büchi B-540 instruments. NMR spectra were recorded on Bruker AV 400 and Bruker AC 300 spectrometers. Chemical shifts are given in parts per million (ppm) and the coupling constants in hertz. Mass spectra were recorded on Bruker Daltonics high-resolution FT-ICR model APEX™ II (4.7 T Magnex cryomagnets supplied with ESI source) and Thermo Finnigan LCQ Advance (APCI). Purifications by column chromatography were performed with Merck silica gel 60 (230–400 mesh for flash chromatography and 70–230 mesh for gravimetric chromatography). All manipulations were carried out under argon atmosphere and the solvents were previously degassed.

Enantioselective HPLC: HPLC enantioseparations were performed by using a stainless steel Chiralpak IA-3 100 × 4.6 mm I.D. (Chiral Technologies Europe, Illkirch, France) column. All chemical solvents for HPLC and spectral-grade solvents were purchased from Aldrich (Italy) and used without further purification.

The analytical HPLC apparatus consisted of a PerkinElmer (Norwalk, CT, USA) 200 lc pump equipped with a Rheodyne (Cotati, CA, USA) injector, a 20 µL sample loop, a HPLC Dionex CC-100 oven (Sunnyvale, CA, USA), and a Jasco (Jasco, Tokyo, Japan) Model CD 2095 Plus UV/CD detector. The signal was acquired and processed by Clarity software (DataApex, Prague, The Czech Republic). Low-temperature chromatography was performed by placing the column in an MGWLauda Cryostat (Messgerate-Werk Lauda, Germany) and employing a 1 m connecting capillary placed in the ethylene glycol cooling bath, to ensure thermal equilibration of the mobile phase.

Tris[1-(2-methoxynaphthyl)]phosphane (1a): A solution of 1-bromo-2-methoxynaphthalene (1.76 g, 7.4 mmol)^[12] in dry THF (10 mL) was dropped into a suspension of magnesium (189 mg) in THF (3 mL) previously activated with iodine. The addition was completed in 30 min and reflux

was maintained for 2 h. Then a solution of PCl₃ (0.11 mL, 1.23 mmol) in dry THF (1 mL) was added at 0°C to the Grignard solution and the reaction mixture was heated to reflux for 1 h. The solvent was removed under reduced pressure and the residue treated with water (20 mL) and extracted with CH₂Cl₂ (3 × 20 mL). The organic layer was dried and the solvent evaporated to give a residue, which was subjected to chromatography on a silica-gel column (CH₂Cl₂/AcOEt 10/0.5) to give pure **1a** (412 mg, yield 67%). M.p. 177.0–183.5°C (sint. 155.9°C); ¹H NMR (300 MHz, CDCl₃): δ = 8.50–8.38 (m, 3H), 7.75 (t, ³J(H,H) = 8.27 Hz, 6H), 7.34–7.18 (m, 6H), 7.15–7.05 (m, 3H), 3.00 ppm (s, 3H); ³¹P NMR (300 MHz, CDCl₃): δ = -58.32 ppm (s); APT NMR (300 MHz; CDCl₃): δ = 159.62 (s), 136.61 (d, ²J(C,P) = 23.24 Hz), 130.23 (s), 129.38 (d, ³J(C,P) = 4.75 Hz), 128.14 (s), 126.39 (d, ³J(C,P) = 30.56 Hz), 125.95 (s), 123.22 (s), 119.96 (d, ¹J(C,P) = 18.26 Hz), 115.21 (s), 56.46 ppm (s); MS (EI): *m/z* (%): 502 (2) [M]⁺, 473 (75).

Tris[1-(2-ethoxy-6-sulfonaphthyl)]phosphane (1c): Tris[1-(2-ethoxy)naphthyl]phosphane (**1b**)^[3] 2.4 g, 4.41 mmol) was added to oleum with 20% SO₃ (3.6 mL) at 0°C and the reaction mixture was stirred at room temperature for 3 h. A solution of NaOH pellets (5.28 g, 132 mmol) in deoxygenated water (44 mL) was added to neutralize the solution while keeping the temperature between -5 and 0°C. MeOH (30 mL) was added to the mixture, the insoluble salts were eliminated by filtration, and the filtrate was evaporated to dryness under reduced pressure. The solid residue was triturated with AcOEt to give the sodium salt of the title product (5.5 g), which was dissolved in MeOH (15 mL) and filtered through a C100 MBH Purolite column to give **1c**, which was triturated with AcOEt (2.75 g, yield 80%). M.p. 282°C; ¹H NMR (300 MHz, CD₃OD): δ = 8.44 (d, ³J(H,H) = 9.29 Hz, 3H), 8.45 (brt, 3H), 7.81 (d, ³J(H,H) = 9.00 Hz, 3H), 7.76 (dd, ³J(H,H) = 8.9, ⁴J(H,H) = 1.7 Hz, 3H), 7.65 (dd, ³J(H,H) = 9.2 Hz, ⁴J(H,H) = 5.83 Hz, 3H), 4.16–4.00 (m, 6H), 3.45–3.39 (m, 3H), 0.65 ppm (t, ³J(H,H) = 7.0 Hz, 9H); ³¹P NMR (300 MHz, CD₃OD): δ = -39.69 ppm; APT NMR (400 MHz, CD₃OD): δ = 164.70 (s), 142.98 (s), 140.65 (s), 135.89 (d, ²J(C,P) = 7.27 Hz), 129.77 (d, ³J(C,P) = 10.29 Hz), 128.43 (s), 127.86 (s), 123.68 (d, ³J(C,P) = 10.63 Hz), 115.93 (d, ³J(C,P) = 7.21 Hz), 99.13 (d, ¹J(C,P) = 97.31 Hz), 67.30 (s), 14.18 ppm (s); HRMS (ESI⁺): *m/z* calcd for C₃₆H₃₄O₁₂S₃P (+1): 785.09445; found 785.09417 [M+H]⁺.

1-Bromo-2,6-diethoxynaphthalene: A solution of NBS (1.55 g, 8.69 mmol) in AcOH (100 mL) was added to a solution of 2,6-diethoxynaphthalene^[13] (1.88 g, 8.69 mmol) in CHCl₃ (100 mL); the reaction mixture was stirred at room temperature for 3 h and then water (100 mL) was added. The organic layer was separated and washed with 5% NaHCO₃ solution (2 × 100 mL), dried (MgSO₄), and the solvent removed under reduced pressure. The yellowish residue was subjected to chromatography on an alumina column (eluent: hexane/AcOEt 22/1) and then on a silica-gel column (eluent: hexane/CH₂Cl₂ 8/2). The first fractions eluted gave the 1,5-dibromo-2,6-diethoxynaphthalene (76 mg, yield 2.3%). M.p. 127°C. The 1-bromo-2,6-diethoxynaphthalene was recovered in the last fractions (0.725 g, yield 28%). M.p. 104–105°C; ¹H NMR (300 MHz, CDCl₃): δ = 8.13 (d, ³J(H,H) = 9.31 Hz, 1H), 7.65 (d, ³J(H,H) = 8.99 Hz, 1H), 7.22 (dd, ³J(H,H) = 9.29 Hz, ⁴J(H,H) = 2.46 Hz, 1H), 7.21 (d, ³J(H,H) = 8.96 Hz, 1H), 7.07 (d, ⁴J(H,H) = 2.46 Hz, 1H), 4.22 (q, ³J(H,H) = 6.99 Hz, 2H), 4.14 (q, ³J(H,H) = 6.99 Hz, 2H), 1.50 (t, ³J(H,H) = 6.93 Hz, 3H), 1.48 ppm (t, ³J(H,H) = 6.88 Hz, 3H); APT NMR (300 MHz; CDCl₃): δ = 155.95 (s), 151.73 (s), 130.99 (s), 128.52 (s), 127.89 (s), 127.31 (s), 120.53 (s), 116.34 (s), 110.21 (s), 106.82 (s), 66.25 (s), 63.59 (s), 15.11 (s), 14.78 ppm (s); MS (FAB⁺): *m/z* (%): 296 (100), 294 (77) [M]⁺, 216 (30).

Tris[1-(2,6-diethoxynaphthyl)]phosphane (1d): A solution of 1-bromo-2,6-diethoxynaphthalene (0.8 g, 2.71 mmol) in dry THF (7 mL) was dropped into a suspension of magnesium (65.9 mg) in THF (3 mL), previously activated with iodine. The mixture was refluxed until magnesium disappeared, a solution of PBr₃ (0.064 mL, 0.678 mmol) in dry THF (1 mL) was added at room temperature, and the reaction mixture heated to reflux for 24 h. The solvent was removed under reduced pressure and the residue treated with AcOEt (5 mL). The insoluble solid was recovered by filtration to give **1d** in a good purity (0.37 g, yield 80%). M.p. 190.2–191.3°C (sint. 188.1°C); ¹H NMR (300 MHz, CDCl₃): δ = 8.33 (dd, ³J-

(H,H)=9.20 Hz, 4J (H,P)=4.06 Hz, 3H), 7.60 (d, 3J (H,H)=9.01 Hz, 3H), 7.07–6.96 (m, 6H), 6.82 (dd, 3J (H,H)=9.36 Hz, 5J (H,P)=2.62 Hz, 3H), 4.06 (q, 3J (H,H)=6.56 Hz, 6H), 3.73–3.50 (m, 6H), 1.41 (t, 3J (H,H)=6.88 Hz, 9H), 0.51 ppm (t, 3J (H,H)=6.91 Hz, 9H); ^{31}P NMR (300 MHz, CDCl_3): δ = –55.36 ppm (s); APT NMR (300 MHz, CDCl_3): δ = 157.05 (d, 2J (C,P)=6.04 Hz), 154.67 (s), 132.35 (d, 2J (C,P)=19.25 Hz), 130.24 (d, 3J (C,P)=3.77 Hz), 128.79 (s), 128.45 (d, 3J (C,P)=25.59 Hz), 120.40 (d, 1J (C,P)=20.30 Hz), 118.11 (d, 4J (C,P)=2.26 Hz), 115.43 (s), 107.02 (s), 64.61 (s), 63.23 (s), 14.86 (s), 13.91 ppm (s); MS (ESI): m/z (%): 677.5 [$M+H$] $^+$.

(–)-(2*S*,3*S*)-2,3-Dihydro-2,3-dimethylnaphtho[2,3-*b*]-1,4-dioxin: Dry K_2CO_3 (8 g, 57.9 mmol) and a solution of (2*R*,3*R*)-butanediol ditosylate^[14] (20 g, 50.1 mmol) in DMF (50 mL) were added to a solution of 2,3-dihydroxynaphthalene (8 g, 0.05 mmol) in DMF (50 mL). The reaction mixture was heated at 100 °C for 24 h, then the mixture was poured into water (150 mL) and extracted with CH_2Cl_2 (3 × 150 mL). The organic layers were washed with water, dried (Na_2SO_4), and the solvent removed under reduced pressure to give a brown residue, which was treated with AcOEt (20 mL) to give a brownish solid (6.3 g, yield 59%). M.p. 122 °C; ^1H NMR (200 MHz, CDCl_3): δ = 7.64 (m, 2H), 7.28 (m, 3H), 3.97 (m, 2H), 1.41 ppm (dd, 3J (H,H)=4.31 Hz, 4J (H,H)=1.83 Hz, 6H); APT NMR (300 MHz; CDCl_3): δ = 144.49 (s), 129.93 (s), 126.79 (s), 124.39 (s), 112.35 (s), 75.06 (s), 17.64 ppm (s); MS (EI): m/z (%): 215 (17) [$M+H$] $^+$, 214 (100) [M] $^+$, 185 (27), 171 (41), 160 (65); [α] 25_D = –1.48° (c = 0.1 in CHCl_3).

(–)-(2*S*,3*S*)-5-Bromo-2,3-dihydro-2,3-dimethylnaphtho[2,3-*b*]-1,4-dioxin: NBS (5.15 g, 28.9 mmol) was added to a solution of (2*S*,3*S*)-2,3-dimethylnaphtho[2,3-*b*]-1,4-dioxene (6.2 g, 29.0 mmol) in 50% $\text{CHCl}_3/\text{AcOH}$ (60 mL); the reaction mixture was stirred at room temperature for 15 h and then water (50 mL) was added. The organic layer was separated and washed with 5% NaHCO_3 solution (2 × 50 mL), dried (Na_2SO_4), and the solvent removed under reduced pressure to give a brown oil. A solid (1.6 g) separated on addition of hexane and the mother liquors, evaporated to dryness gave a residue which was subjected to chromatography on a silica-gel column (hexane/ CH_2Cl_2 98/2). (2*S*,3*S*)-5,10-Dibromo-2,3-dimethylnaphtho[2,3-*b*]-1,4-dioxene was eluted in the initial fractions, and then the title compound was recovered (2.5 g, yield 49%). M.p. 84 °C; ^1H NMR (300 MHz, CDCl_3): δ = 8.14 (d, 3J (H,H)=8.57 Hz, 1H), 7.69 (d, 3J (H,H)=8.57 Hz, 1H), 7.48–7.38 (m, 1H), 7.38–7.31 (m, 1H), 7.30 (s, 1H), 4.10–3.97 (m, 2H), 1.54 (d, 3J (H,H)=6.20 Hz, 3H), 1.47 ppm (d, 3J (H,H)=6.20 Hz, 3H); APT NMR (300 MHz; CDCl_3): δ = 143.82(s), 129.48 (s), 128.21 (s), 126.76 (s), 125.68 (s), 125.18 (s), 124.63 (s), 111.62 (s), 111.34 (s), 107.07 (s), 75.55 (s), 74.49 (s), 17.06 (s), 17.01 ppm (s); MS (EI): m/z (%): 294 (99) [M] $^+$, 292 (100) [M] $^+$, 265–263 (15), 251–249 (25), 240–238 (53); [α] 25_D = –1.07° (c = 0.1 in CHCl_3).

Tris(5-((2*S*,3*S*)-2,3-dihydro-2,3-dimethylnaphtho[2,3-*b*]-1,4-dioxinyl))-phosphane [(P_{res})-2*b* and (M_{res})-2*b*]: A 1.7 M solution of *t*BuLi in pentane (3.27 mL, 5.56 mmol) was dropped into a solution of (–)-(2*S*,3*S*)-5-bromo-2,3-dihydro-2,3-dimethylnaphtho[2,3-*b*]-1,4-dioxin (815 mg, 2.78 mmol) in dry THF (5 mL) at –68 °C, and then PCl_3 (0.06 mL, 0.70 mmol) was added at room temperature and the reaction mixture heated to reflux for 20 h. The solvent was removed under reduced pressure and the residue dissolved in CH_2Cl_2 , washed with 9% HCl solution, dried (MgSO_4), and the solvent removed under reduced pressure to give a residue which was subjected to chromatography on a silica-gel column (heptane/AcOEt 9/1). The first fraction eluted gave some (2*S*,3*S*)-2,3-dimethylnaphtho[2,3-*b*]-1,4-dioxene (233 mg). The following fractions gave a 1/2 mixture of the $P_{\text{res}}/M_{\text{res}}$ diastereoisomers of 2*b* (92 mg, yield: 20%). ^1H NMR (500 MHz, CDCl_3): δ = 8.41 (dd, 3J (H,H)=8.25 Hz, 4J (H,P)=3.25 Hz, minor diast. 3H), 8.33 (dd, 3J (H,H)=8.25 Hz, 4J (H,P)=4.25 Hz, major diast. 3H), 7.62 (d, 3J (H,H)=8.50 Hz, major diast. 3H), 7.60 (d, 3J (H,H)=8.00 Hz, minor diast. 3H), 7.30–7.24 (m, major diast. 3H + minor diast. 3H), 7.21 (s, major diast. 3H + minor diast. 3H), 7.14 (t, 3J (H,H)=7.75 Hz, major diast. 3H), 7.10 (t, 3J (H,H)=8.00 Hz, minor diast. 3H), 3.74 (d quart., 3J (H,H)=6.50 Hz, 3J (H,H)=7.36 Hz, major diast. 3H), 3.61–3.49 (m, minor diast. 6H), 3.05 (d quart., 3J (H,H)=6.50 Hz, 3J (H,H)=7.36 Hz, major diast. 3H), 1.23 (d, 3J (H,H)=6.00 Hz, minor diast. 9H), 1.17 (d, 3J (H,H)=6.50 Hz, major diast. 9H),

0.54 (d, 3J (H,H)=6.00 Hz, major diast. 9H), 0.51 ppm (d, 3J (H,H)=6.00 Hz, minor diast. 9H); ^{31}P NMR (500 MHz, CDCl_3): δ = –56.42 (s, major diast.), –56.85 ppm (s, minor diast.); APT NMR (500 MHz, CDCl_3): δ = 146.00 (d, 2J (C,P)=2.26 Hz, major diast.), 145.87 (d, 2J (C,P)=5.66 Hz, minor diast.), 143.52 (s, major diast.), 143.21 (s, minor diast.), 132.41 (d, 2J (C,P)=19.74 Hz, minor diast.), 131.89 (d, 2J (C,P)=23.27 Hz, major diast.), 129.60 (d, 3J (C,P)=5.41 Hz, major diast.), 129.34 (d, 3J (C,P)=4.53 Hz, minor diast.), 126.77 (two superimposed s of both diast.), 126.30 (d, 3J (C,P)=25.15 Hz, minor diast.), 125.88 (d, 3J (C,P)=28.68 Hz, major diast.), 123.56 (s major diast.), 123.51 (two superimposed s of minor diast.), 123.35 (s, major diast.), 118.00 (d, 1J (C,P)=18.36 Hz, minor diast.), 117.85 (d, 1J (C,P)=20.63 Hz, major diast.), 112.94 (s, minor diast.), 112.60 (s, major diast.), 74.31 (s, minor diast.), 74.20 (s, major diast.), 73.78 (s, minor diast.), 73.63 (s, major diast.), 17.04 (s, major diast.), 16.94 (s, minor diast.), 15.89 ppm (superimposed s of both diast.); MS (EI): m/z (%): 670 (100) [M] $^+$, 530 (13), 458 (15). The last fractions gave a mixture of the phosphane oxides corresponding to 2*b* (40 mg).^[12]

4-Bromo-2,2-dimethyl-naphtho[2,3-*d*]-1,3-dioxole: NBS (0.68 g, 3.83 mmol) was added to a solution of 2,2-dimethylnaphtho[2,3-*d*]-1,3-dioxole^[15] (0.77 g, 3.83 mmol) in 50% $\text{CHCl}_3/\text{AcOH}$ (30 mL). The reaction mixture was stirred at room temperature for 3 h, water (50 mL) was added, and the organic layer was separated and washed with saturated K_2CO_3 solution (3 × 10 mL), dried (Na_2SO_4), and the solvent removed under reduced pressure to give a residue, which was subjected to chromatography on a silica-gel column (hexane). The pure title compound was obtained as a viscous oil (0.75 g, yield 70.2%). ^1H NMR (300 MHz, CDCl_3): δ = 8.086 (d, 3J (H,H)=8.40 Hz, 1H), 7.66 (d, 3J (H,H)=8.40 Hz, 1H), 7.50–7.30 (m, 2H), 7.04 (s, 1H), 1.83 ppm (s, 6H); ^{13}C NMR (300 MHz, CDCl_3): δ = 146.92 (s), 146.93 (s), 130.78 (s), 128.50 (s), 127.06 (s), 125.08 (s), 124.99 (s), 124.71 (s), 103.17 (s), 97.12 (s), 25.97 ppm (s); MS (EI): m/z (%): 280 (96) 278 (98) [M] $^+$, 265 (73) 263 (78), 240 (97) 238 (100).

Tris[4-(2,2-dimethyl-naphtho[2,3-*d*]-1,3-dioxolyl)]phosphane (3): A 1.6 M solution of *t*BuLi in hexane (3.2 mL, 5.38 mmol) was added to a solution of 4-bromo-2,2-dimethylnaphtho[2,3-*d*]-1,3-dioxole (0.75 g, 2.69 mmol) in THF (14 mL) at –60 °C. After 30 min a solution of PCl_3 (0.059 mL, 0.672 mmol) in THF (1 mL) was added. The reaction mixture was heated to reflux for 27 h. The solvent was evaporated under reduced pressure, then CH_2Cl_2 (50 mL) and 8% HCl solution (70 mL) were added. The organic layer was separated and dried over Na_2SO_4 . The solvent was evaporated to dryness to give a residue, which was purified by chromatography on a silica-gel column (hexane/AcOEt 9/1). Compound 3 was obtained as a colorless solid (0.18 g, yield 43%). It crystallized as a conglomerate from AcOEt, and thus both enantiomers could be recovered. Racemate: M.p. 333–337 °C; ^1H NMR (300 MHz, CDCl_3): δ = 8.33–8.26 (m, 3H), 7.58 (d, 3J (H,H)=7.60 Hz, 3H), 7.28–7.17 (m, 6H), 6.96 (s, 3H), 1.34 (s, 9H), 0.76 ppm (s, 9H); ^{31}P NMR (300 MHz, CDCl_3): δ = –61.59 ppm (s); APT NMR (300 MHz, CDCl_3): δ = 151.45 (s), 146.92 (d, 3J (C,P)=8.23 Hz), 132.82 (d, 2J (C,P)=22.19 Hz), 130.44 (s), 127.00 (d, 3J (C,P)=28.22 Hz), 123.87 (s), 123.60 (s), 116.42 (s), 107.80 (d, 1J (C,P)=105.96 Hz), 104.29 (s), 25.66 (s), 24.59 ppm (s); MS (EI): m/z (%): 628 (100) [M] $^+$, 629 (43) [$M^+ + H$], 613 (15).

Electrochemical measurements: The cyclic voltammetric study was performed at scan rates typically ranging from 0.02 to 1 V s^{-1} in HPLC-grade acetonitrile solutions at 0.00025–0.001 M concentration in each substrate, deaerated by N_2 bubbling, with 0.1 M tetrabutylammonium perchlorate (TBAP, Fluka) as supporting electrolyte at room temperature. The ohmic drop was compensated by the positive-feedback technique.^[16] The experiments were carried out by using an AUTOLAB PGSTAT potentiostat (EcoChemie, The Netherlands) run by a PC with GPES software. The glassy carbon working electrode (AMEL, surface area = 0.071 cm^2) was cleaned by diamond powder (Aldrich, diameter = 1 μm) on a wet cloth (STRUERS DP-NAP); the counterelectrode was a platinum disk; the reference electrode was an aqueous saturated calomel electrode, having in our working medium a difference of –0.385 V versus the Fc^+/Fc couple (the intersolvental redox potential reference currently recommended by IUPAC).^[17]

Crystal data for (2S,3S)-5-bromo-2,3-dimethyl-naphtho[2,3-b]-1,4-dioxene: $C_{14}H_{13}BrO_2$, $M_r = 293.15$; monoclinic, $P2_1$; $a = 9.251(2)$, $b = 16.497(3)$, $c = 9.398(2)$ Å; $\beta = 117.33(2)^\circ$; $V = 1274.2(5)$ Å³; $Z = 4$; $\rho_{\text{calcd}} = 1.528$ g cm⁻³; $\mu(\text{MoK}\alpha) = 3.213$ cm⁻¹; $F(000) = 592$; pale yellow prism, $0.24 \times 0.28 \times 0.30$ mm; Bruker APEX2000 diffractometer; 14200 data collected, 5521 unique, $R_{\text{int}} = 0.0276$, 4020 with $I_0 > 2\sigma(I_0)$. The structure was solved by direct methods^[18] and refined anisotropically by full-matrix least-squares techniques based on F^2 .^[19] H atoms were in calculated positions. The asymmetric unit contains two independent molecules of **3**, both with the same 2S,3S conformation, with their minimum inertial axes antiparallel, simulating a centrosymmetric group. The final refinement was on 307 parameters and 1 restraint. The final results, on all and observed reflections, were $R_1 = 0.0585$ and 0.0370 , $wR_2 = 0.0952$ and 0.0873 , GOF 1.028; residues on the final map were from -0.74 to 0.60 e Å⁻³. The absolute configuration was established by anomalous dispersion [Flack parameter = 0.008(13)].

Crystal data for 3: $C_{39}H_{33}O_6P$, $M_r = 628.62$; trigonal, $R3$; $a = 11.6355(12)$, $c = 21.069(2)$ Å; $V = 2470.3(3)$ Å³; $Z = 3$; $\rho_{\text{calcd}} = 1.268$ g cm⁻³; $\mu(\text{MoK}\alpha) = 0.130$ cm⁻¹; $F(000) = 990$; colorless rhombohedron, $0.15 \times 0.26 \times 0.50$ mm; Bruker APEX2000 diffractometer; 48507 data collected, 1982 unique, $R_{\text{int}} = 0.0426$, 1877 with $I_0 > 2\sigma(I_0)$. The structure was solved by direct methods^[18] and refined anisotropically by full-matrix least-squares techniques based on F^2 .^[19] H atoms were in calculated positions. The molecule of **3** lies on a crystallographic threefold axis. The final refinement was on 141 parameters and 1 restraint. The final results, on all and observed reflections, were $R_1 = 0.0314$ and 0.0273 , $wR_2 = 0.0759$ and 0.0704 , GOF 1.120; residues on the final map were from -0.10 to 0.20 e Å⁻³. The absolute configuration was established by anomalous dispersion [Flack parameter = $-0.03(10)$].

CCDC-872695 (2,3-dimethylnaphtho[2,3-b]-1,4-dioxene) and CCDC-872696 (**3**) contain the supplementary crystallographic data for this paper. These data can be obtained free of charge from The Cambridge Crystallographic Data Centre via www.ccdc.cam.ac.uk/data_request/cif.

Molecular modeling calculations: All molecular modeling calculations were performed on a PC equipped with 3.40 GHz Intel Pentium 4 CPU, 2 GB of RAM, and Windows 2000 Professional. Ground- and transition-state geometries of all tris-aryl substituted and model phosphanes considered in the theoretical study of this work, corresponding to the energetic findings reported in Table S10 of the Supporting Information, were initially optimized in vacuo at the SCF level by the semiempirical AM1 method and then refined by the hybrid Hartree-Fock/DFT method B3LYP with 6-31G(d) basis set, as implemented in SPARTAN 04 (Wavefunction Inc. 18401 Von Karman Avenue, Suite 370, Irvine, CA 92612, USA). For all obtained transition states a single imaginary frequency was identified, always corresponding to the correct vibration suitable to allow the related stereomutation (i.e., P inversion or the M_0 process). The CD spectrum of phosphane **3** was simulated by performing calculations on the above DFT optimized structures of (P_{aaa})-**3** and (M_{aaa})-**3**, that is, the only two conformers among the four belonging to the M_{res} enantiomer of **3** that calculations predicted to be populated. The CD assessments were carried out in chloroform by the BLYP method with QZ4P large-core basis set, as implemented in the ADF package v. 2007.01. The set options were: single-point calculation; chloroform solvation computed with the conductor like screening model (COSMO), with the cavity defined according to the solvent-excluding surface (SES) algorithm; 40 singlet and triplet excitations; diagonalization method: Davidson. The average CD spectrum was obtained by weighting the CD profiles assessed for (P_{aaa})-**3** and (M_{aaa})-**3** on the calculated BP values of the relevant conformations.

Simulation of dynamic chromatograms: Simulations of experimental dynamic chromatograms were performed by using the Auto-DHPLC-y2k laboratory-made computer program,^[6m-u] which implements both stochastic and theoretical plate models^[6a-l] and can take into account all types of first-order interconversion as well as tailing effects. In the present paper, simulations of dynamic chromatograms of phosphanes **1a** and **1d** were carried out by stochastic model, and those of phosphane **1b** by theoretical plate model. In all cases tailing effects were taken into consideration.

Acknowledgements

Work supported by MIUR PRIN-2007 "Catalizzatori innovativi a base di metalli di transizione per sintesi mirate chemo- e stereo-selettive" and by CNR. T.B. thanks the Dipartimento di Chimica Organica e Industriale of the University of Milano for hospitality.

- [1] P. Finocchiaro, D. Gust, K. Mislow, *J. Am. Chem. Soc.* **1973**, *95*, 8172; P. Finocchiaro, D. Gust, K. Mislow, *J. Am. Chem. Soc.* **1974**, *96*, 2165; J. D. Andose, K. Mislow, *J. Am. Chem. Soc.* **1974**, *96*, 2168; P. Finocchiaro, D. Gust, K. Mislow, *J. Am. Chem. Soc.* **1974**, *96*, 2176; P. Finocchiaro, D. Gust, K. Mislow, *J. Am. Chem. Soc.* **1974**, *96*, 3198; P. Finocchiaro, D. Gust, K. Mislow, *J. Am. Chem. Soc.* **1974**, *96*, 3205; C. Foces-Foces, F. H. Cano, M. Martínez Ripoll, R. Faure, C. Roussel, R. M. Claramunt, C. López, D. Sanz, J. Elguero, *Tetrahedron: Asymmetry* **1990**, *1*, 65.
- [2] T. Benincori, V. Bonometti, R. Cirilli, P. R. Mussini, A. Marchesi, M. Pierini, T. Pilati, S. Rizzo, F. Sannicolò, *Chem. Eur. J.* **2012**, paper immediately preceding this one, DOI: 10.1002/chem.201201180.
- [3] T. Benincori, A. Marchesi, T. Pilati, A. Ponti, S. Rizzo, F. Sannicolò, *Chem. Eur. J.* **2009**, *15*, 86.
- [4] T. Benincori, R. Cirilli, R. Ferretti, F. La Torre, O. Piccolo, L. Zanitti, *Chromatographia* **2002**, *55*, 25; N. G. Andersen, M. Parvez, R. McDonald, B. A. Keay, *Can. J. Chem.* **2004**, *82*, 145; M. Thimmaiah, R. L. Luck, S. Fang, *The Open Organic Chemistry Journal* **2008**, *2*, 1.
- [5] R. Ferretti, A. Mai, B. Gallinella, L. Zanitti, S. Valente, R. Cirilli, *J. Chromatogr. A* **2011**, *1218*, 8394.
- [6] a) R. A. Keller, J. C. Giddings, *J. Chromatogr.* **1960**, *3*, 205; b) R. Kramer, *J. Chromatogr.* **1975**, *107*, 241; c) V. Schurig, W. Bürkle, *J. Am. Chem. Soc.* **1982**, *104*, 7573; d) W. Bürkle, H. Karfunkel, V. Schurig, *J. Chromatogr.* **1984**, *288*, 1; e) J. Veciana, M. I. Crespo, *Angew. Chem.* **1991**, *103*, 85; *Angew. Chem. Int. Ed. Engl.* **1991**, *30*, 74; f) M. Jung, *QCPE Bull.* **1992**, *12*, 52; g) K. Cabrera, M. Jung, M. Fluck, V. Schurig, *J. Chromatogr. A* **1996**, *731*, 315; h) J. Oxelbark, S. Allenmark, *J. Org. Chem.* **1999**, *64*, 1483; i) O. Trapp, G. Schoetz, V. Schurig, *Chirality* **2001**, *13*, 403; j) C. Wolf, *Chem. Soc. Rev.* **2005**, *34*, 595; k) O. Trapp, *Anal. Chem.* **2006**, *78*, 189; l) I. D'Acquarica, F. Gasparrini, M. Pierini, C. Villani, G. Zappia, *J. Sep. Sci.* **2006**, *29*, 1508; m) F. Gasparrini, L. Lunazzi, A. Mazzanti, M. Pierini, K. M. Pietrusiewicz, C. Villani, *J. Am. Chem. Soc.* **2000**, *122*, 4776; n) C. Dell'Erba, F. Gasparrini, S. Grilli, L. Lunazzi, A. Mazzanti, M. Novi, M. Pierini, C. Tavani, C. Villani, *J. Org. Chem.* **2002**, *67*, 1663; o) F. Gasparrini, S. Grilli, R. Leardini, L. Lunazzi, A. Mazzanti, D. Nanni, M. Pierini, M. Pinamonti, *J. Org. Chem.* **2002**, *67*, 3089; p) A. Dalla Cort, F. Gasparrini, L. Lunazzi, L. Mandolini, A. Mazzanti, C. Pasquini, M. Pierini, R. Rompietti, L. Schiaffino, *J. Org. Chem.* **2005**, *70*, 887; q) R. Cirilli, R. Ferretti, F. La Torre, D. Secci, A. Bolasco, S. Carradori, M. Pierini, *J. Chromatogr. A* **2007**, *160*, 1172; r) R. Cirilli, R. Costi, R. Di Santo, F. La Torre, M. Pierini, G. Siani, *Anal. Chem.* **2009**, *81*, 3560; s) W. Cabri, I. D'Acquarica, P. Simone, M. Di Iorio, M. Di Mattia, F. Gasparrini, F. Giorgi, A. Mazzanti, M. Pierini, M. Quaglia, C. Villani, *J. Org. Chem.* **2011**, *76*, 1751; t) W. Cabri, I. D'Acquarica, P. Simone, M. Di Iorio, M. Di Mattia, F. Gasparrini, F. Giorgi, A. Mazzanti, M. Pierini, M. Quaglia, C. Villani, *J. Org. Chem.* **2011**, *76*, 4831; u) L. Lunazzi, M. Mancinelli, A. Mazzanti, M. Pierini, *J. Org. Chem.* **2010**, *75*, 5927.
- [7] R. D. Baechler, K. Mislow, *J. Am. Chem. Soc.* **1970**, *92*, 3090.
- [8] D. S. Marynick, D. A. Dixon, *J. Phys. Chem.* **1982**, *86*, 914.
- [9] J. M. Lehn, B. Munsch, *Mol. Phys.* **1972**, *23*, 91.
- [10] W. Egan, K. Mislow, *J. Am. Chem. Soc.* **1971**, *93*, 6205.
- [11] T. Benincori, A. Marchesi, P. R. Mussini, T. Pilati, A. Ponti, S. Rizzo, F. Sannicolò, *Chem. Eur. J.* **2009**, *15*, 94.
- [12] P. Chhattise, A. V. Ramaswamy, S. B. Waghmode, *Tetrahedron Lett.* **2005**, *18*, 2837.
- [13] T. Nemoto, G. Konishi, *Polym. J.* **2008**, *40*, 651.
- [14] X. Li, K. D. Robinson, P. P. Gaspar, *J. Org. Chem.* **1996**, *61*, 7702.

- [15] H.-W. Zhang, Q.-H. Meng, Z.-G. Zhang, *Chin. J. Chem.* **2008**, *26*, 2098.
- [16] A. J. Bard, L. R. Faulkner, *Electrochemical Methods. Fundamentals and Applications*, Wiley, New York, **2002**, 648.
- [17] a) G. Gritzner, J. Kuta, *Pure Appl. Chem.* **1984**, *56*, 461; b) G. Gritzner, *Pure Appl. Chem.* **1990**, *62*, 1839.
- [18] M. C. Burla, M. Camalli, B. Carrozzini, G. L. Cascarano, C. Giacovazzo, G. Polidori, R. Spagna, *J. Appl. Crystallogr.* **2003**, *36*, 1103.
- [19] G. M. Sheldrick, *Acta Crystallogr. Sect. A* **2008**, *64*, 112.


Received: April 6, 2012

Revised: August 3, 2012

Published online: ■■■■, 0000

Residual Stereoisomerism

*S. Rizzo, T. Benincori, V. Bonometti,
R. Cirilli, P. R. Mussini, M. Pierini,
T. Pilati, F. Sannicolò* ■■■■-■■■■*

 **Steric and Electronic Effects on the Configurational Stability of Residual Chiral Phosphorus-Centered Three-Bladed Propellers: Tris-aryl Phosphanes**



Residual antipodes of a tris-aryl phosphane were isolated in enantiopure state for the first time, and absolute configurations assigned to them by single-crystal anomalous X-ray diffraction analysis. A detailed computational investigation was carried out to clarify the helix reversal mechanism. Calculations indicated that the low configurational stability of tris-aryl phosphanes can be attributed to unexpectedly easy phosphorus pyramidal inversion (see figure).